NANO LETTERS

2007
Vol. 7, No. 2
227−232

Nanoscale Current Imaging of the Conducting Channels in Proton Exchange Membrane Fuel Cells

David A. Bussian, James R. O'Dea, Horia Metiu, and Steven K. Buratto*

California Nanosystems Institute (CNSI) and Department of Chemistry and Biochemistry, University of California, Santa Barbara, California 93106-9510

Received May 22, 2006; Revised Manuscript Received December 12, 2006

ABSTRACT

The electrochemically active area of a proton exchange membrane fuel cell (PEMFC) is investigated using conductive probe atomic force microscopy (CP-AFM). A platinum-coated AFM tip is used as a nanoscale cathode in an operating PEMFC. We present results that show highly inhomogeneous distributions of conductive surface domains at several length scales. At length scales on the order of the aqueous domains of the membrane, ∼50 nm, we observe single channel electrochemistry. *I*−*V* curves for single conducting channels are obtained, which yield insight into the nature of conductive regions across the PEM. In addition, we demonstrate a new characterization technique, phase current correlation microscopy, which gives a direct measure of the electrochemical activity for each aqueous domain. This shows that a large number (∼60%) of the aqueous domains present at the surface of an operating Nafion membrane are inactive. We attribute this to a combination of limited aqueous domain connectivity and catalyst accessibility.

We present a new type of atomic force microscopy (AFM) measurement used to examine the hydrophilic channels in a Nafion membrane. The system of interest is a Nafion membrane pressed on a carbon cloth gas-diffusion electrode on which platinum catalyst was deposited. The carbon cloth is exposed to hydrogen. A platinum-coated AFM tip is brought into contact with the exposed membrane surface wherein it functions as a nanoscale cathode. As the tip is scanned over the surface it passes over hydrophilic and hydrophobic domains in the Nafion membrane. Current is detected when the tip is positioned over a hydrophilic domain which crosses the membrane and has a catalytic particle at its end. This is due to the formation of protons, at the carbon cloth side of the cell, and the reduction of oxygen at the tip. This current is a direct measure of the charge-transfer processes at the electrodes and proton transport within the aqueous domains. A map of the electrochemically active regions of the Nafion surface is constructed by scanning the platinum tip over the surface. The ability to measure the distribution and activity of the electrochemically active domains in situ is critical to understanding the transport properties of the membrane and the accessibility of the catalyst. Previous work has indirectly measured the connectivities of the aqueous domains through a Nafion membrane.[1,2] Both of these studies use directed electrochemistry through aqueous channels as a measure of the number density of membrane spanning aqueous domains. In the work presented here the channel connectivity is measured directly and explicitly via current imaging which detects the location of the aqueous domains responsible for proton transport. These are domains that cross the membrane and have a catalyst particle at the end opposite to the tip. The proton exchange membrane fuel cell (PEMFC) has been the subject of considerable interest over the last several decades because of its potential as an alternative energy source. The typical PEMFC is composed of a proton exchange membrane (PEM) which is sandwiched on either side by a porous carbon based electrode on which one deposits Pt/Ru or Pt catalyst particles. For a cell to operate successfully (i.e., supply electricity), the fuel (e.g., hydrogen or methanol) must reach the catalytic particles at the interface between aqueous domains in the PEM and the carbon electrode and the protons formed at the anode must traverse the aqueous domains of the PEM and reach the catalyst at the cathode. The perfluorosulfonate ionomer Nafion (see Figure 1a) is the polymer used most frequently to make fuel cell membranes. A Nafion membrane consists of an interpenetrating network of nanoscale aqueous domains surrounded by a semirigid fluorocarbon backbone.[3] The size and extent of the aqueous domains or "channels" control proton diffusion, and it is one of the factors controlling the maximum current densities supported by a cell.[4] Furthermore, the topology of the aqueous domains directly affects catalyst and membrane utilization. Only channels that cross the membrane and have a catalytic particle at each end generate current in a cell. Recent studies

* Corresponding author: buratto@chem.ucsb.edu.

10.1021/nl061170y CCC: $37.00
Published on Web 01/26/2007

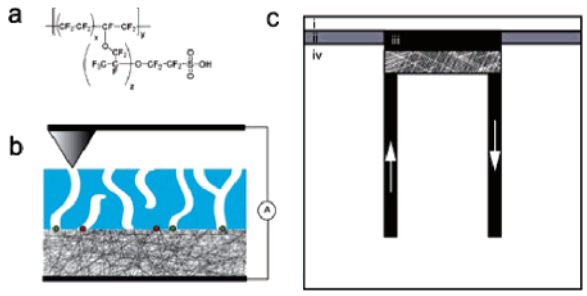

Figure 1. (a) Chemical structure of Nafion 117 where $x \sim 6.5$, $y \sim 230$, and $z = 1$. (b) The configuration of the half MEA and the conductive tip in experimental apparatus. (c) Nano fuel cell flow: (i) Nafion 117 membrane; (ii) insulating layer; (iii) Pt-loaded carbon electrode; (iv) copper base.

of catalyst placement have shown that the catalytic particles "at each end" can be within a diffusion-mediated region near the aqueous domain termed the reaction zone.[5,6] This reaction zone can extend up to 10 nm from the catalytic particle.[6] Catalytic particles trapped under a hydrophobic domain outside the reaction zone, or those located near a channel that does not have a catalyst particle within the reaction zone at the opposite electrode, are wasted. The unused particles and channels add to the cost of the cell without contributing to its performance.[7]

Previous efforts at understanding catalyst utilization have focused primarily on the impact of catalyst loading conditions on fuel cell performance.[8] In addition to catalyst placement, the chemical morphology of the PEM interface plays a critical role in catalyst utilization. The spatial heterogeneity of the PEM surface of a variety of polymers has been investigated with both scan probe techniques[9−11] and various spectroscopies.[12−15] Furthermore, the number and distribution of membrane spanning aqueous domains has been recently probed[1,2] via electrochemical methods.

This Letter describes the use of conducting AFM to obtain high spatial resolution images of the current passing through each channel of the membrane, in an electrochemically active fuel cell. This technique allows *direct* observation of the hydrophilic domains responsible for proton creation and transport. We measure the electrochemical activity of a working half MEA, one channel at a time, and examine the implications of the results to catalyst utilization, active channel density, and the role of interfacial water layers.

AFM has been shown to be a powerful tool for nanoscale surface modification,[16] electrochemistry,[17] and characterization.[18,19] Previous studies[15,20,21] of Nafion membranes have reported measurements of the interfacial electrical properties using various forms of conductive probe AFM (CP-AFM). In the work of O'Hayre et al.,[20,21] nanoscale impedance measurements were made on an active PEMFC, which detailed oxidation−reduction reaction kinetics on the tip. For the first time, these experiments provided insight into the faradaic processes at the cathode. In particular, they were able to quantitatively measure the rates of the oxidation reduction reaction occurring at a nanoscale electrode (CP-AFM tip) in an active PEMFC. Earlier work by Kanamura et al.[15] used a combination of in situ FT-IR spectroscopy

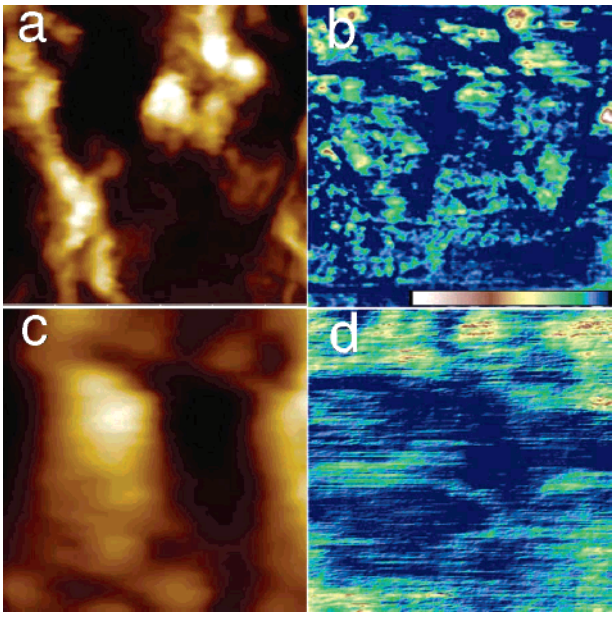

Figure 2. AFM images of an active hydrogen fuel cell: (a) height (*z*-scale 75 nm) and (b) current (*z*-scale 20 pA, color bar with blue at 0 and maximum as white) regions of a 1 μm × 1 μm region; (c) height (*z*-scale 10 nm); (d) current (*z*-scale 5 pA) images of a 500 nm × 500 nm region taken from the center of the scan in (a).

and surface potential microscopy (SPoM) to show the swelling of interfacial aqueous domains with increased water concentration. In this case, a CoCr probe was used to measure the surface potential above an inactive (no fuel source) Nafion membrane mounted to a bare platinum electrode. The results presented in this work are distinguished from previous studies because they are focused on providing a quantitative measure of the *spatial distribution* of electrochemically active aqueous domains in a PEMFC. This allows us to determine, with high resolution, the distribution and characteristics of the proton channels responsible for PEMFC performance.

Figure 1b depicts a general schematic of the sample geometry used in this study. A half membrane electrode assembly (MEA) is prepared by pressing a Nafion 117 membrane onto a Pt catalyst loaded carbon electrode (see Experimental Section for details). This assembly is then mounted onto a copper flow cell as shown in Figure 1c. Once assembled, the flow cell is loaded into the AFM apparatus (Veeco Multimode, Nanoscope IIIa). The anode compartment is exposed to hydrogen gas (99.999% pure) at 5 ccm. A Pt/Ir coated AFM tip (Nanoworld, 225 μm long, $k_s \sim 2.8$ N/m) is brought into contact with the half MEA, at which point the tip becomes a nanoscale cathode. A cathodic bias of 500 mV is generally required to observe significant current, which we attribute to the electric resistance of the hydrophilic channel and the faradaic processes at the tip. Current derived from the coupled redox reactions is collected through the CP-AFM tip and passed through a series of high gain current preamplifiers (Veeco, Tunneling AFM(TUNA)). As the tip is scanned along the polymer interface, the surface height and the cathodic current are measured simultaneously.

Figure 2a shows a 1 μm × 1 μm topographic image of the Nafion surface with its corresponding current image in

Figure 2b. The current image shows an inhomogeneous distribution of electrochemically active domains at the membrane surface. Inspection of numerous current images yields qualitatively similar distributions of active surface domains as shown in Figure 2b. To compare the current observed in these measurements with those of operating bulk PEMFCs, we generated a histogram of the number of points that exhibited a given current. These currents were converted to a current density by considering the tip−sample force, tip shape, and nanoscale sample hardness (obtained from O'Hayre et al.[21]). This histogram shows that the active domains have an average current density of approximately 35 mA/cm^2 with a peak of nearly 300 mA/cm^2, which falls within the operating range of bulk cells.[22] A magnified, 500 nm × 500 nm, topographic and current scan taken from the center region of Figure 2a is displayed in parts c and d of Figure 2, respectively. The high current domains in Figure 2d appear to have no strong correlations to topographic features. This is consistent with previous tapping mode AFM (TMAFM) work[9−11] which shows no correlation between topographic features and aqueous domains. At this scan size, tip convolution becomes a significant issue and regions below ∼50 nm cannot be unambiguously resolved. In addition, the water meniscus formed at the apex of the tip in conjunction with any excess surface water further decreases the spatial resolution. The fact that the conductive regions appear to be both limited by the size of the tip and well isolated is strong evidence for the observation of single conductive surface domains. The domain sizes represented fit well with previous experimental and theoretical predictions of hydrophilic pore diameter.[4] Thus it is likely that these isolated domains represent at most a small number of electrochemically active hydrophilic domains and may, in some cases, represent single, electrochemically active domains.

The ability to resolve isolated conductive surface domains lends further insight into the larger area distributions of current observed in Figure 2b. Each of the high current domains observed in Figure 2b is likely composed of many unresolved conductive channels. The inhomogeneous distribution of conductive surface domains on length scales over hundreds of nanometers shows evidence of single active domain clustering throughout the surface. At first this appears inconsistent with previous TMAFM results which show a roughly uniform distribution of aqueous domains. However, one must recall that the underlying structure of the membrane (aqueous domain connectivity) and catalyst accessibility place additional constraints on the ability for given aqueous domains at the surface to support electrochemistry. This technique cannot distinguish between these two effects. However, the observation of regions which exhibit no significant electrochemical activity directly highlights the intrinsic under utilization of the membrane interface.

In addition to mapping the spatial distribution of electrochemically active proton channels, CP-AFM of PEMFCs permits the collection of single-point $I-V$ curves for the active cell. $I-V$ curves are obtained by maintaining a constant tip/sample force and then varying the tip/sample bias while measuring the cathodic current. This gives the

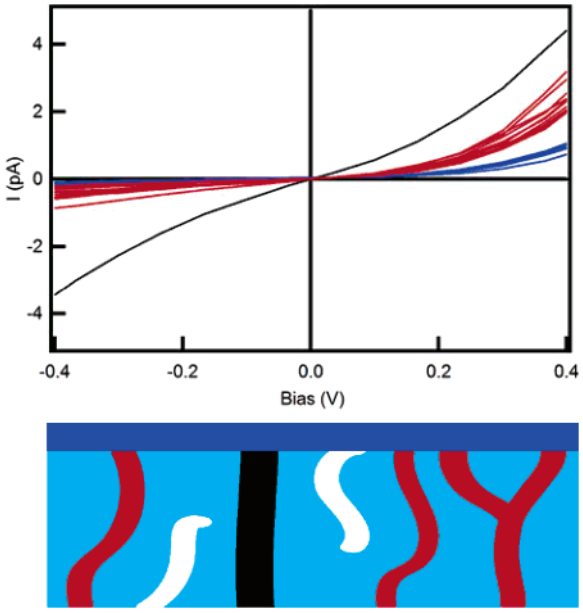

Figure 3. (top) $I-V$ curves measured point by point over the surface. The plot displays cathodic (tip collected) current vs tip/sample potential. (bottom) Schematic model of general aqueous domain topology according to polarization grouping where blue represents a surface aqueous layer, red contiguous membrane spanning domains, and black membrane defects (pinholes) or very large domains.

closed circuit current for the nanocell. Figure 3 depicts 25 curves taken on a 5 μm × 5 μm grid with 1 μm point to point spacing. The bias sweep runs from −400 to 400 mV to stay below the water electrolysis threshold. Inspection yields three obvious curve groupings distinct by their polarization response. The blue curves exhibit minimal response under negative bias and have the lowest current increase with increasing bias. Curves in the red grouping show a slightly increased current response at negative bias and a significant current increase with increasing positive bias. Finally, the black curve shows a nearly symmetric bipolar current response that is larger in magnitude than either the red or blue curves. A sampling of over 200 points which showed measurable current gives the following distribution of site-specific $I-V$ response: <1% black, 70% red, 29% blue. If we consider the total number of points, representing both active and inactive surface regions, the distribution of current response is <0.5% black, 32% red, and 13% blue, where 440 points are sampled over the surface of the sample. This suggests three kinds of surface sites as depicted in the diagram in the bottom of Figure 3. The most common conducting channels correspond to the red curves. The current passing through them at negative bias is small and increases substantially under cathodic bias. The negative bias response is a result of the polarity of the PEMFC where the anodic compartment is nearly pure hydrogen and a reverse reaction (tip as anode) is unfavorable. In contrast, the current increases nonlinearly at cathodic bias as the oxidation reduction reaction becomes more favorable with increasing bias. The current response in the blue curves is similar in form, but significantly less in magnitude, than the red curves. We attribute it to a thin aqueous layer present over large

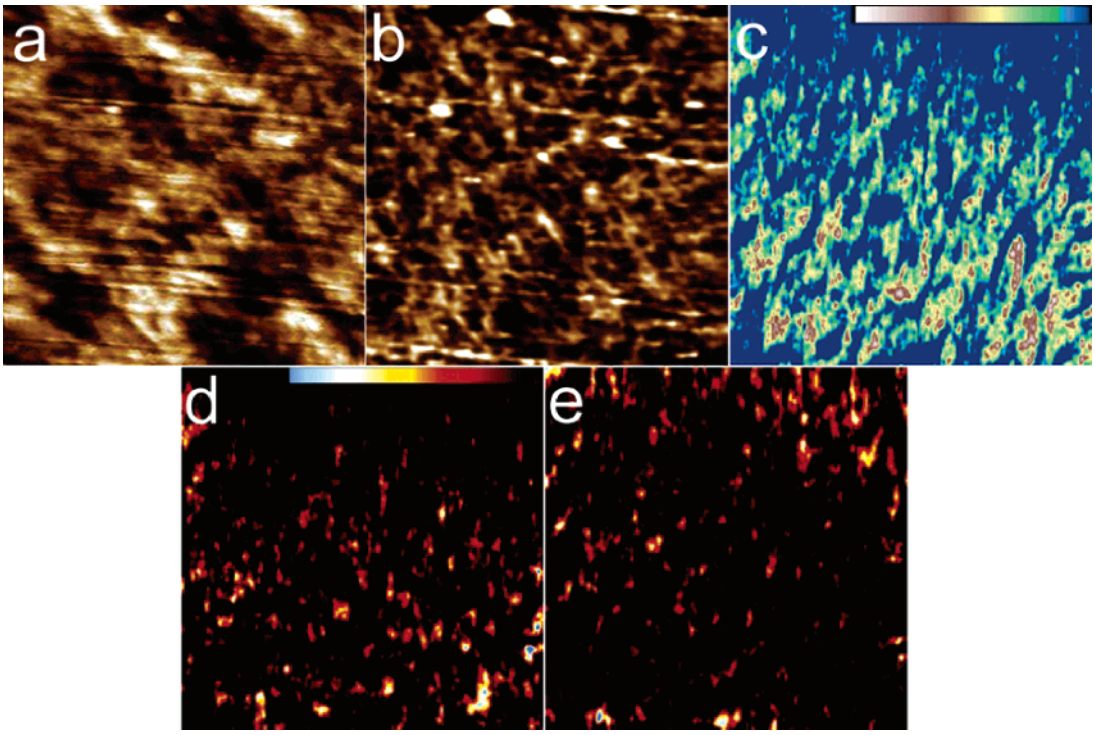

Figure 4. 1 μm × 1 μm AFM images: (a) TMAFM topography (z-scale maximum 10 nm represented in white); (b) TMAFM phase image (z-scale 15°); (c) current image (z-scale maximum 50 pA represented in white); (d) correlation image (C^+) showing regions which contain both aqueous domains and proton conduction (color bar gradient with black at 0 and maximum as blue); (e) anticorrelation (C^-) image showing regions which contain aqueous domains with insignificant proton conduction.

portions of the surface. Proton conduction through this surface layer is less efficient and the measured current is smaller than that of the conducting channels. Measurements on a low water content (~1% by weight) membrane show a substantial drop in the background current further confirming the presence of surface layer proton transport. Finally, the black curves correspond to current through large channels or "pinholes", in which the proton diffuses more rapidly. These sites are primarily distinguished by their bipolar current response which arises due to the ability of oxygen to reach the carbon electrode, and thus, the redox reaction is locally reversible. These sites are relatively rare and are further "masked" by oxygen mass transport through the membrane.

The electrochemical activity of aqueous surface domains can be further probed by examining the correlation between aqueous surface layers and the current derived from them. The PEMFC will only produce current from aqueous domains that cross the membrane and have a catalyst particle within the reaction zone at the anode side. TMAFM shows that roughly 50% or more of the Nafion surface is composed of aqueous domains. Not all surface domains, however, are involved in useful electrochemistry. This is due either to the lack of a catalyst particle at the electrode membrane interface or to an aqueous domain that does not completely transverse the membrane or both. We have developed a new approach which directly correlates the image of the chemical morphology of the surface and the image of the redox current. This is realized by using a dual pass technique called phase current correlation microscopy (PCCM). An initial scan is taken with TMAFM where the topography (Figure 4a) and phase image are recorded (Figure 4b). Then a second, slightly larger scan is taken of the same region in contact mode while measuring the topography and current (Figure 4c) simultaneously. The topography images of the two scans are used as an alignment mask. This allows the current image to be matched pixel by pixel to the same region as in the TMAFM image (see Figure 4c). The phase image displayed in Figure 4b shows a series of light and dark regions corresponding to hydrophobic (fluorocarbon rich) and hydrophilic (sulfonic acid and water rich) domains, respectively. Figure 4c depicts the electrochemically active regions which as discussed earlier are inhomogeneously distributed across the surface. Moreover, the number of conductive regions does not map one-to-one with the surface domains. This is a clear indication that not all aqueous surface domains are electrochemically active and that the distribution of electrochemically active regions in the current image is not simply a result of the distribution of aqueous domains. To facilitate a more direct comparison, a series of cross correlation images were obtained by normalizing phase and current images followed by point-by-point correlation using the following relations

$$C^+(x,y) = |-\phi(x,y)| \times I(x,y) \tag{1a}$$

$$C^-(x,y) = |-\phi(x,y)| \times |-I(x,y)| \tag{1b}$$

where ϕ is the normalized relative phase and I is the normalized current. C^+ is the positive correlation indicating the presence of both an aqueous domain and significant conductance. This is obtained by inverting the phase image such that the hydrophilic domains are positive valued and

then multiplying each point by the corresponding normalized current value. A positive correlation image is shown in Figure 4d. The positive correlation image shows the electrochemically active aqueous domains to be even more sparsely distributed than the conductance image in Figure 4c might suggest. In fact, only 34 ± 8% of the domains observed in the phase image are associated with any appreciable current. The remaining aqueous domains can be seen in the anticorrelation, C^- (see Figure 4e), where nonzero correlation values depict regions with hydrophilic domains that exhibit negligible electrochemical activity. It is instructive to note the top region of the images in parts c and d of Figure 4 where a minimal number of electrochemically active domains are represented in Figure 4c which leads to the high density of anticorrelated domains in Figure 4e. We are currently using PCCM to understand the effects of hydration and membrane preparation on the relative activity of the aqueous domains in the PEM.

In conclusion, we have performed in situ nanoscale current measurements in a polymeric membrane fuel cell using conductive probe atomic force microscopy (CP-AFM). A platinum-coated AFM tip acted as a nanoscale cathode which allowed us to perform electrochemistry through one hydrophilic channel in the membrane of the fuel cell. Only aqueous domains that cross the membrane and have a catalyst at the electrode opposite to the tip produce significant redox current. This makes CP-AFM a useful tool for determining the distribution of electrochemically active aqueous domains in a PEMFC. Single conductive domains are shown to segregate spatially at the nanoscale, due to the spontaneous phase separation of the polymer into hydrophilic channels. At scales larger than the single domains, high current regions are distributed inhomogenously over the surface. This suggests limiting phenomena in the PEMFC including inefficient catalyst accessibility and insufficient aqueous domain connectivity, which decreases the contributions to total cell current to a fraction of the surface. $I-V$ point measurements serve to further characterize the conductive domains yielding three general pathway topologies including surface water, small and intermediate channels, and large channels also termed "pinholes". Finally, PCCM was introduced as a powerful technique for direct determination of the electrochemical activity of aqueous domains. For Nafion 117 PEMFC the correlation between aqueous domains and electrochemical activity was 34 ± 8%.

Material Preparation. Preformed Nafion 117 membranes and Nafion suspensions (1100 e.w.) in alcohols were purchased from Sigma Aldrich. Catalyst loaded (0.5 mg/cm^2) carbon cloth electrodes were obtained from E-Tek, Inc. Nafion 117 membranes were prepared for use by boiling in 0.5 M sulfuric acid and followed by a deionized water rinse for 2 h. Carbon electrodes were coated with a thin film of Nafion by dropcasting from an alcohol suspension. Half membrane electrode assemblies (MEAs) were prepared by hot pressing the membrane to the electrode for 2 min at 130 °C and 6 MPa. Once complete the half MEAs were placed in a humidification chamber and allowed to equilibrate to 43% relative humidity for several days before mounting to the flow cell.

Experimental Methods. To verify that the current measured by CP-AFM was derived from the redox reactions of the hydrogen fuel cell, a number of control experiments were performed to exclude other alternatives. Current was not detected under the each of the following conditions: no hydrogen at anode, no catalyst at anode, non-Pt tip (both Pt/Ir and Pt worked, with Pt/Ir showing higher activity), and membrane equilibrated at 0% relative humidity (∼1% water loading in membrane). This, in conjunction with the unipolar $I-V$ response previously discussed, clearly indicates that the dominant source of current measured by CP-AFM is derived from the oxidation reduction reaction. All conductance measurements were taken with a constant tip/sample force of 52 ± 5 nN. This contact force was maintained during single point $I-V$ measurements by adjusting tip height after every data point. Each $I-V$ curve is an average of a minimum of three measurements per point. Pt-overcoated tips are known to degrade with use. Tips were tested repeatedly and periodically checked with a SEM to chart degradation. PCCM utilized the same intermediate length cantilever for both tapping mode and contact mode measurements. Tapping mode images were taken at ∼75 kHz with a set point amplitude of ∼0.70 versus free space amplitude of 1.2 V.

Comparison of parts c and d of Figure 4 shows a significant fraction, >20%, of all conductive regions are not associated with highly aqueous domains. This is due to the resolution mismatch between TMAFM and CAFM modes. This mismatch is responsible for the difference between the sum of the two correlation plots and the CAFM current image. In other words, the resolution in the correlation plots is dictated by the resolution of TMAFM.

Acknowledgment. Support for this work was provided by an Army Research Office (ARO) MURI.

References

(1) Gargas, D. J.; Bussian, D. A.; Buratto, S. K. *Nano Lett.* **2005**, *5*, 2184−2187.
(2) Chou, J.; McFarland, E. W.; Metiu, H. *J. Phys. Chem. B* **2005**, *109*, 3252−3256.
(3) Paddison, S. J. *J. New Mater. Electrochem. Syst.* **2001**, *4*, 197−207.
(4) Kreuer, K. D.; Paddison, S. J.; Spohr, E.; Schuster, M. *Chem. Rev.* **2004**, *104*, 4637−4678.
(5) Williford, R. E.; Chick, L. A. *Surf. Sci.* **2003**, *547*, 421−437.
(6) O'Hayre, R.; Barnett, D. M.; Prinz, F. B. *J. Electrochem. Soc.* **2005**, *152*, A439−A444.
(7) Chou, J.; Ranasinghe, A.; Shrisudershan, J.; McFarland, E. W.; Buratto, S. K.; Metiu, H. *J. Phys. Chem. B*, in press.
(8) Uchida, M.; Fukuoka, Y.; Sugawara, Y.; Ohara, H.; Ohta, A. *J. Electrochem. Soc.* **1998**, *145*, 3708−3713.
(9) McLean, R. S.; Doyle, M.; Sauer, B. B. *Macromolecules* **2000**, *33*, 6541−6550.
(10) James, P. J.; Antognozzi, M.; Tamayo, J.; McMaster, T. J.; Newton, J. M.; Miles, M. J. *Langmuir* **2001**, *17*, 349−360.
(11) James, P. J.; McMaster, T. J.; Newton, J. M.; Miles, M. J. *Polymer* **2000**, *41*, 4223−4231.
(12) Ayato, Y.; Kunimatsu, K.; Osawa, M.; Okada, T. *J. Electrochem. Soc.* **2006**, *153*, A203−A209.
(13) Affoune, A. M.; Yamada, A.; Umeda, M. *J. Power Sources* **2005**, *148*, 9−17.
(14) Malevich, D.; Zamlynny, V.; Sun, S. G.; Lipkowski, J. *Z. Phys. Chem.—Int. J. Res. Phys. Chem. Chem. Phys.* **2003**, *217*, 513−525.

(15) Kanamura, K.; Morikawa, H.; Umegaki, T. *J. Electrochem. Soc.* **2003**, *150*, A193−A198.
(16) Piner, R. D.; Zhu, J.; Xu, F.; Hong, S. H.; Mirkin, C. A. *Science* **1999**, *283*, 661−663.
(17) Schneegans, O.; Moradpour, A.; Boyer, L.; Ballutaud, D. *J. Phys. Chem. B* **2004**, *108*, 9882−9887.
(18) Samori, P. *J. Mater. Chem.* **2004**, *14*, 1353−1366.
(19) Kelley, T. W.; Granstrom, E. L.; Frisbie, C. D. *Adv. Mater.* **1999**, *11*, 261.
(20) O'Hayre, R.; Lee, M.; Prinz, F. B. *J. Appl. Phys.* **2004**, *95*, 8382−8392.
(21) O'Hayre, R.; Feng, G.; Nix, W. D.; Prinz, F. B. *J. Appl. Phys.* **2004**, *96*, 3540−3549.
(22) Whittingham, M. S.; Savinell, R. F.; Zawodzinski, T. *Chem. Rev.* **2004**, *104*, 4243−4244.

NL061170Y